Phase Response Curves of Square Wave Bursting Neurons: A Modeling Approach

Ikemefuna Agbanusi
Department of Applied Mathematics, New Jersey Institute of Technology

Abstract

We study the phase response properties of the PD neuron in the Stomato-gastric Ganglion (STG). We use model equations describing a square wave bursting oscillation to define and analyze the phase response dynamics for weak and strong perturbations. In the real and model neurons, we observe that the PRC saturates with amplitude. We show that for strong perturbations, much of the phase response is due either to the addition of spikes in the active phase, the deletion of spikes or the termination of the active phase of the oscillation. Discontinuities are also present in the PRCs we obtain. This discontinuity may be related to the method of obtaining the PRCs. In trying to understand the onset of these phenomena, we use a phase model to determine approximate conditions under which square shaped current pulses cause spike addition and deletion. We break apart the phase response over the active and silent phases of the oscillation and, in the companion paper, describe algorithms to predict the full phase response from both pieces. We also discuss here two possible methods to understand the phase response in the active phase. We also use ideas from geometric singular perturbation theory and dynamical systems theory to describe burst truncation and in particular it is shown that the saturation of the PRC can be explained using the calcium dynamics for strong inhibition in the active phase and strong excitation in the silent. Furthermore, the discontinuity in the PRC for strong excitation is shown to be a 'topological' property in the sense that it cannot be removed.

Introduction

The experiment of phase resetting has a long history which dates back to the extensive work done by Winfree [19] on certain biological and chemical oscillators. The experiments were originally carried out on the circadian rhythm, the idea being to characterize responses of the period of the cycle/rhythm to precisely timed stimulus. The phase resetting or response curve (PRC) is then a plot of the 'response' of the period against the timing of the stimulus that elicited the 'response'. The notion of a 'response' will be fixed later on in this paper. In short, however it measures the response of the oscillator period to timed inputs.

Mathematically, the biological oscillator is modeled by a set of ordinary deterministic differential equations which possesses a stable periodic solution. Under this setting, one can view the impulse of current as causing excursions from this periodic solution. The assumption of stability implies that these perturbations die out and the oscillator returns to its original periodic motion. The PRC can be shown to be determined by what is known as 'isochrons' [11]. Isochronous points are those whose time evolution 'look alike' and thus have essentially the same 'timing'. Dynamical systems theory, which is the qualitative theory of ordinary differential equations yields relevant characterizations of the isochrons of periodic motions. In sections of this paper we shall draw on elements of dynamical systems theory to explain the PRC of the biological oscillator which we consider and model.

The notion of a PRC is not just a long winded formalism and it is a useful notion when one considers networks of biological oscillators. If we know the PRC of the individual oscillators then presumably, given any input into the oscillators we know how they shall respond and hence we know the future states of the oscillators. Thus given any network of oscillators, once we figure out the network connectivity or coupling which describes how the oscillators in the network 'talk' or send signals/inputs to each other, as well as know the individual PRCs, then, in theory, we can determine the individual and also the collective behavior of the network. In this paper, we are not primarily concerned with network behavior of any kind. It would be untrue though to say that network behavior is not part of our problem situation. We study the PRC of a neural oscillator which is part of a network of oscillators in the Stomato-gastric Ganglion (STG) of the crab, *Cancer Borealis.* Very little information is needed about the STG to understand this paper since we study one neuron kernel in isolation from the network. This isolation was achieved by applying pharmacological agents which block the synapses of the neuron and hence block inputs to the neuron. However, as we have indicated, no harm will be done if one keeps the big picture (i.e. network) in mind in trying to understand the implications of our experiments and results.

The kernel we study is the anterior burster/pyloric dilator (AB-PD) neuron kernel which is the pacemaker kernel for the pyloric rhythm of the STG. Both cells are electrically coupled and it is for this reason that we treat them as a single unit in so far as the synaptic

coupling between the PD and other cells in the network is removed. The PD neuron is an endogenous bursting neuron. Its membrane potential profile is depicted in (Fig 1). Its membrane potential has periods of fast spiking activity (active phase) and slow quiet activity (rest phase). We compute the PRC by injecting current pulses of different amplitude into the biological and model (i.e. mathematical) neurons. The PRC of this pacemaker kernel of the STG has been studied quite extensively for various types of stimuli [1, 8]. It has been shown that there is a saturation of the PRC with varying amplitude of stimulus [1]. In computing their PRCs, they use synaptic conductance pulses via Dynamic clamp as opposed to the current pulses we utilize here. Nonetheless, with the use of current pulses, the PRCs of the biological and model PD neuron still shows saturation with amplitude. Such saturation has relevant implications for the global network function [1].

Apart from the saturation of the PRC with amplitude, we made some other interesting observations. For larger stimulus input the main causes of changes in the period of the oscillator is either one of spike deletion, spike addition and burst truncation. Burst truncation is a termination, by a perturbatory input, of the active phase of the oscillation. Spike deletion (addition) is a shortening (lengthening) of the active phase of the oscillator by the decrease (increase) in the number of spikes in the active phase of the oscillation. These notions will be fixed in later sections of this paper. Our description will provide an explanation of the results obtained in [8] where strongly coupled biological and engineered (artificial) neurons were considered. They observed anti-phase locked (1-1 locking) of the biological and engineered neuron. The reason will become evident with our discussion of burst truncation.

Much theoretical work has been done [17] describing schemes to determine the stability of neural networks composed of simple integrate and fire (IF) neurons or some Type 1 neurons. Recall that Type 1 neurons are neurons for which the frequency at the onset of oscillation can be arbitrarily small. These works rely heavily on the phase variable and notion of phase reduction, concepts which do not generalize easily to higher dimensional relaxation oscillators, or at least not for the strong perturbations typically considered for bursting neurons where the PRC saturate with amplitude and for which phase resetting is caused by burst truncation by the strong inputs. Our goal then is to give mechanisms, based on the intrinsic dynamics of the oscillator, how these phenomena come about. We also consider a novel approach of determining the PRC over different parts of the oscillator and then piecing them together to explain the full PRC. For instance, we compute the PRC using the spike shifting in the active phase of the oscillator and then use this to predict the actual PRC of the full oscillation. This has the added advantage of breaking the PR dynamics into two parts each of which can be understood independently. This method will of course have its domain of application as well as its limitations which we try to elucidate. The paper is divided into (five) sections. First we present our experimental and numerical methods for determining the PRC; we also briefly describe the mathematical model used. Next, we discuss the experimental and numerical observations. We then focus on the phenomena of spike deletion, spike addition and burst truncation and we mathematically derive conditions (some necessary, some sufficient) for spike deletion and spike addition using ideas from the theory of ordinary differential

equations. Next we define and describe burst truncation using results from geometric singular perturbation theory. We then quantify our novel approach to computing the PRC and qualify it using earlier results.

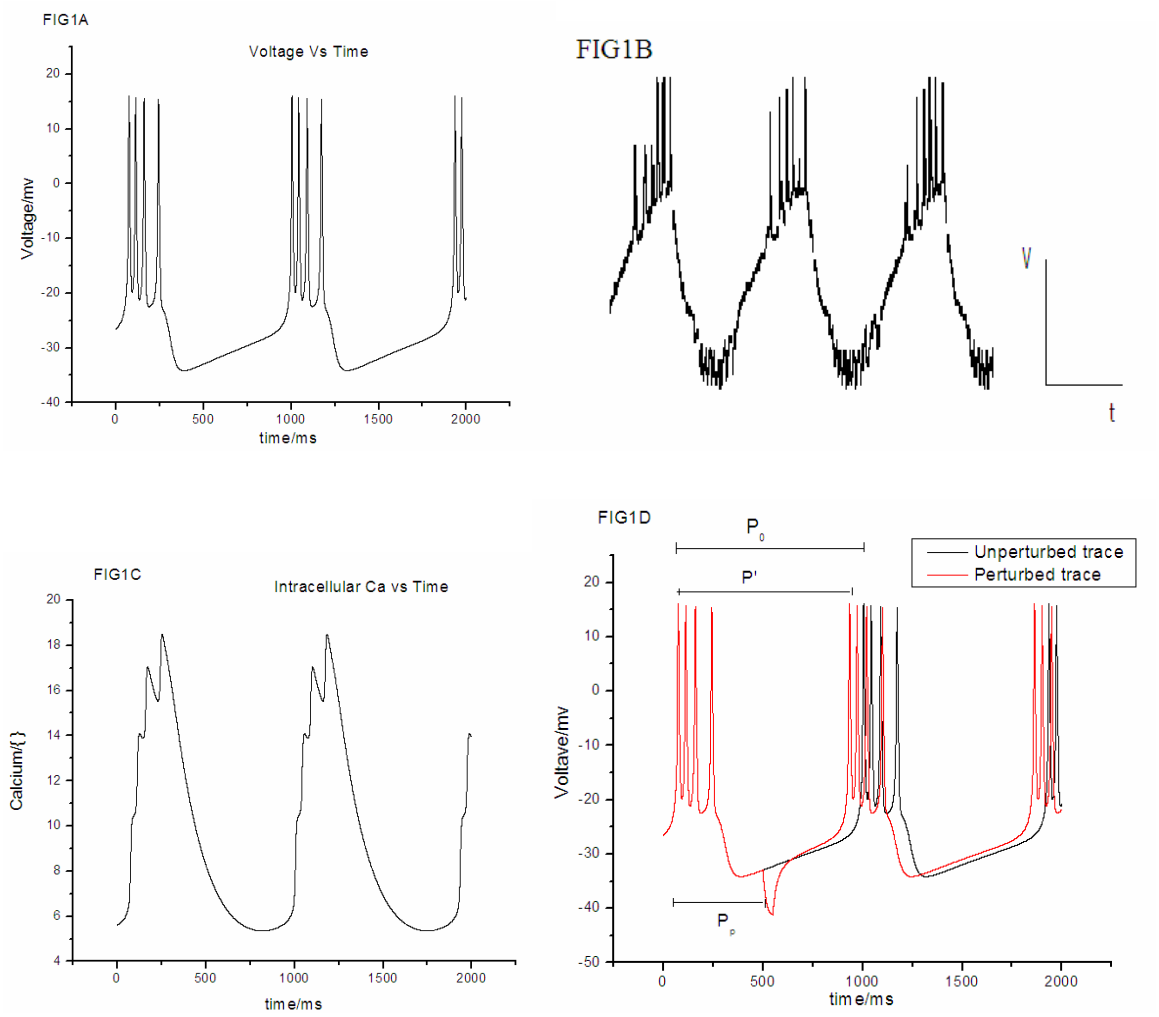

FIG 1: (**A)** Trace of membrane potential of the model (mathematical) neuron is shown. (**B**) Trace of membrane potential of the PD Neuron with LP-PD synapse in tact. The average period of the oscillation is about 1s. (**C**) Trace of intracellular Ca^{2+} concentration for the model neuron. (**D**) Plot showing various terms in the definition of the PRC.

SECTION I

Methods and Definitions

The PRC: The free running oscillator is assumed to have an intrinsic period of P_0 as measured from the start of one active phase or burst to the start of the next burst as illustrated in Fig 1d. Phase zero is arbitrarily set to the start of the burst. The timing of the perturbation is measured from the zero phase and is denoted P_p as shown in Fig 1d and for this input the stimulus phase or what we call here the phase of perturbation is defined as P_p/P_0. For a single perturbation, we define the phase response to be the period change, i.e. the difference between the time of the start of the burst after the stimulus input and the time of the burst assuming there was no input. This difference is simply $\Delta P = P_0 - P'$ as indicated in Fig 1d. If a perturbation causes the next burst to begin earlier than it would have, the perturbation is said to have advanced the phase and it is clear that $\Delta P > 0$. This situation is that shown in Fig 1d. If the perturbation causes the burst to begin at a later time than it would have, the stimulus is said to have delayed the phase and in this case $\Delta P < 0$ holds. A PRC is then a plot of the normalized period change ($\Delta P / P_0$) versus the phase of perturbation defined above. This same methodology was used irrespective of whether it was a biological or model neuron concerned. We offer slight variations of this definition in a later section especially as concerns the model neurons.

Remark 1: An important assumption that we make in the experimental and numerical determination of PRCs is that the biological oscillator has an observable reference event (RE). In the case of a tonic spiking cell this could be the peak (or trough) of an action potential. In the case of a bursting cell it could be the crossing of some arbitrary but fixed membrane potential in a specified direction or it could be the *n*th spike in a burst. It should be clear that different experimentalist can choose different REs and that the PRC is dependent on the RE chosen [7]. What is not so clear is that, but we will show later, is that the choice of RE may lead to misleading results.

***Physiological Recordings*:** Cancer Borealis we purchased and maintained in sea water at about 12 ºC until used. The Stomatogastric nervous systems (STNSs) were dissected out and pinned on Petri dishes coated with Sylgard and the STGs we de-sheathed with fine forceps to enable entry by electrodes into the cells. All through the experiments the cells were kept healthy and maintained at specific temperature and ion concentrations by continuously passing cold saline throughout the dish.
Extra cellular recordings were made using stainless steel pin electrodes in Vaseline wells around certain motor nerves. The Vaseline well served to create a potential difference between the region immediately surrounding a motor nerve and the rest of the dish. The signals were amplified by a differential amplifier. Intra cellular recordings were made

using salt (ion) filled glass micro-electrodes whose resistances were in the range of 18 – 40 MΩ. Both intra cellular and extra cellular voltage traces were digitized and recorded using Clampex. The PD and lateral pyloric (LP) neuron were identified using their voltage traces and matching them against the pyloric rhythm. The LP to PD synapse, the only synapse into the pacemaker kernel, was blocked using either TTX a neurotoxin that blocks spike mediated components of action potentials, or blocked by hyperpolarizing the LP neuron.
The PRC was computed by in house software. To inject the current, the software tracked the state of the voltage variable by detecting when it crossed some fixed threshold with positive slope. The time of first crossing was determined and the perturbation was sent at the required phase as measured from the prior crossing of the threshold. The next input was spaced at least 4 burst periods away from the previous one to ensure that the neuron returned as close as possible to its intrinsic periodic motion and also in order to prevent entraining the oscillator. The voltage current traces were saved and analyzed offline. The perturbations were injected at ten equally spaced points in the cycle corresponding to a phase resolution of 0.1. This enabled us to perform more experiments and average the PRC over all of them.

Remark 2: Slight complications arise because the period of the real biological neuron is not constant. The complication is two fold because, presumably, the period of the oscillation is changing already and it is difficult to estimate just which changes in period, if any, are due to the stimulus and not to the already intrinsically varying period. The other relevant implication of the changing period is that the normalizations done in computing the PRC are not done using the same period since it depends on the period just before that in which the perturbation occurs. The only way we knew to side step these complications was to use data from experiments that showed as little variation as possible. We would like to point out, however, that it was never possible to get absolutely constant periods.

Model Equations: In our mathematical model we use adopt a reduced model of a square wave burster as in [12]. The model is essentially a Morris-Lecar type model with an addition of slowly varying calcium currents which is responsible for creating bursting behavior as proved using geometric singular perturbation theory described in [3]. The model equations are the following:

$$\begin{aligned} C\frac{dv}{dt} &= (I_{ext} - I_{Ca} - I_K - I_L + ms(t-\psi)) \\ \frac{dw}{dt} &= \rho(w_\infty(v) - w) \big/ \tau_w(v) \\ \frac{dCa}{dt} &= \varepsilon(-\mu I_{Ca}(v) - Ca) \end{aligned} \qquad (1)$$

V represents the membrane potential; *w* represents a phenomenological variable which represents the gating process for the ions passing through the membrane and *Ca* represents the aforementioned intracellular calcium. *C* is the membrane capacitance and I_i represents external, calcium, potassium or leak current depending on *i*. The full equations and parameters are described in Appendix A and the XPP code with which it is run is also described in the same appendix. The relevant fact here is that the parameter ε is assumed small in the model and it is responsible for the 'slowness' of the calcium equation. We shall exploit this separation of time scales later to help describe certain aspects of the model. The last term on the right in the first equation represents our perturbation term which is implemented in our numerical simulations as a step function the height of which is the amplitude of the perturbation/stimulus and the width corresponds to the duration of the stimulus given by the parameters *m* and ψ respectively. The PRC of the model neuron was computed as outlined above for the biological neuron.

Mathematical Aspects of PRCs: PRCs are mostly computed for biological oscillators and the idea is to measure how the oscillator reacts to discrete disturbances. In our case the biological oscillator is the bursting PD cell of the STG in the Crab. We have assumed that the cell can be modeled as a differential equation/dynamical system which we write as:

$$\dot{X} = F(X) \tag{2}$$

Or equivalently by the flow:

$$\Psi(X,t) \tag{3}$$

Where $D_t \Psi\big|_{t=0} = F(X)$ (D_t denotes partial differentiation w.r.t to time) and the flow essentially carries us from some initial position to some state after time *t*. Here $X \in M$ where *M* is a smooth manifold. In our case, $M = \mathbb{R}^n$. More so, we assume that (2) has a stable limit cycle which we denote by Γ. Furthermore we assume that Γ is asymptotically orbitally stable. In this case, the existence of isochrons (stable manifolds) is guaranteed for all points on Γ. The additional assumption of normal hyperbolicity ensures that the attraction in a direction normal to Γ is greater than the tangential attraction. The existence of isochrons is then essentially a theorem of dynamical systems. We shall soon briefly describe isochrons.

In addition we assume that the perturbed system can be written as:

$$\dot{X} = F(X,m)$$

Here $m \in \mathbb{R}$ denotes the perturbation, positive values signify excitatory perturbations while negative values signify inhibitory perturbations. Clearly, $|m|$ gives the amplitude of the perturbation. We also adopt the standard definition of phase as the time elapsed from the reference event. Note that Γ is a periodic solution to (1) and has period T. For trajectories close to Γ we expect that the time between the reference events will approach T. We adopt the standard definition for the phase map $\Theta : M \to S^1$ where S^1 is the unit

circle and Θ defines the phase or asymptotic phase of a point in M depending on whether the point is on Γ or in an appropriately defined neighborhood of Γ. We also adopt the standard definition of isochron [2, 7] and the stable manifold of an invariant set [4]. As pointed out above, the existence of isochrons is a theorem of dynamical systems when the limit cycle is assumed to be normally hyperbolic. Also they foliate the neighborhood of the limit cycle [6].

As we mentioned earlier, we assume that there is an RE and that this reference event is triggered in some determinate way (i.e. it is not random). In most PRC experiments the RE is triggered when the membrane potential crosses some predetermined threshold or when the membrane potential reaches its peak. It should be clear that the threshold defines an n-1 dimensional hyper-plane in phase space. In the case of using the voltage peak as a reference event, the RE is also determined by a hyper-surface of some sorts. In this case it is the null surface of the v equations since on this surface $\frac{dv}{dt} = 0$ in accordance with the idea of a peak in voltage. In determining the PRC we used a combination of these two prescriptions. We require that the voltage cross a threshold with a positive slope. This defines a plane in the region of phase space where v is increasing. In both cases the RE events determine and are uniquely determined by a manifold in phase space. As in [7] we call this manifold the detection manifold (DM). More precisely the DM is a connected subset of M that intersects Γ at exactly one point and is defined such that if a trajectory $X(t)$ crosses the DM, the RE is triggered. It is important to note that the DM is not necessarily an isochron even though in the experiments and numerical simulations we assign the phase 0 or 1 as soon as a trajectory crosses the DM.

SECTION II

Results and Observations

We summarize here the main results of our experiments and numerical simulations. We begin first be depicting some of the typical numerical PRCs obtained for weak Fig 2 a-b and strong Fig 2c-d perturbation amplitudes of perturbation of the model and biological neuron. The PRCs for weak perturbations can typically be dissected into three regions. The first is the active phase in which the oscillator is the most sensitive. In the middle phases, the phase response is typically small and the oscillator becomes more sensitive in the late phase. In the weak perturbation regime, the PRC of the inhibitory stimulus is a reflection of that of the excitatory stimulus about the *x*-axis. For strong perturbations, however, this symmetry is lost Fig 2c-d. From our definitions above, we see that inhibition causes advance in the early and late phases and little delay or no change at all in the middle of the oscillation.

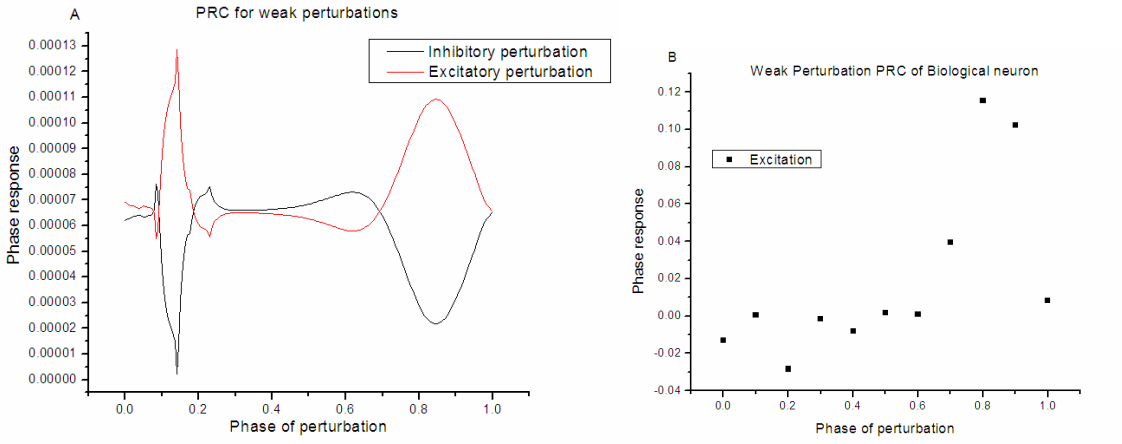

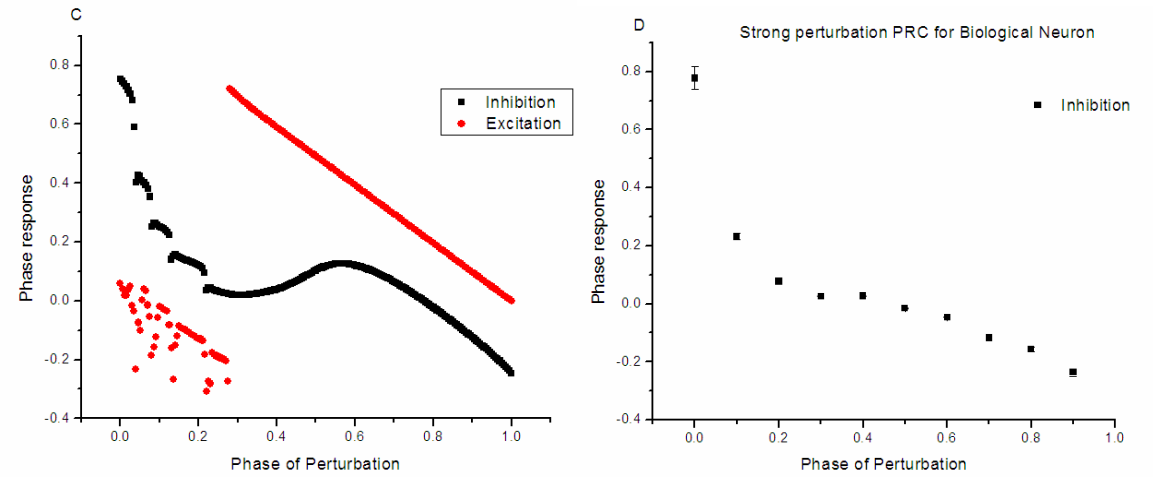

FIG 2: (**A**) Plot of the PRC of the model neuron for weak excitatory and inhibitory perturbations. (**B**) PRC of biological neuron for weak perturbation (0.5nA). Note the general qualitative agreement with the model (Red trace in (b)). (**C**) Strong perturbation PRC for the model neuron. There is a sharp discontinuity in the red trace at the point corresponding to the end of the active phase. (**D**) Strong perturbation PRC of the model. It agrees qualitatively with the model (Black trace in (c)).

Saturation of the PRC with Amplitude: We also observe that the PRC saturates with the amplitude of the perturbation for both the model and biological neuron as shown Fig 3a-b. In order to facilitate a more direct comparison we normalize the PRC by the amplitude of the perturbation. These results are shown in Fig 3c. We see from this figure that, in the active phase of the oscillation, weak perturbations (red and black curves) cause delays while strong perturbations cause advances in this regime. In mid phase there is qualitative agreement of the PRC for all the amplitudes considered while there is some substantial deviation at late phase. This observation thus marks out the active and late phases as regions of interest. We shall study the PRC of the active phase more in depth later. Shown also (Fig 3e) is a plot of the phase response of the model neuron as a function of the phase of perturbation and the perturbation amplitude. The different PRCs can thus be obtained by passing relevant planes across this surface and extracting the curve of intersection.

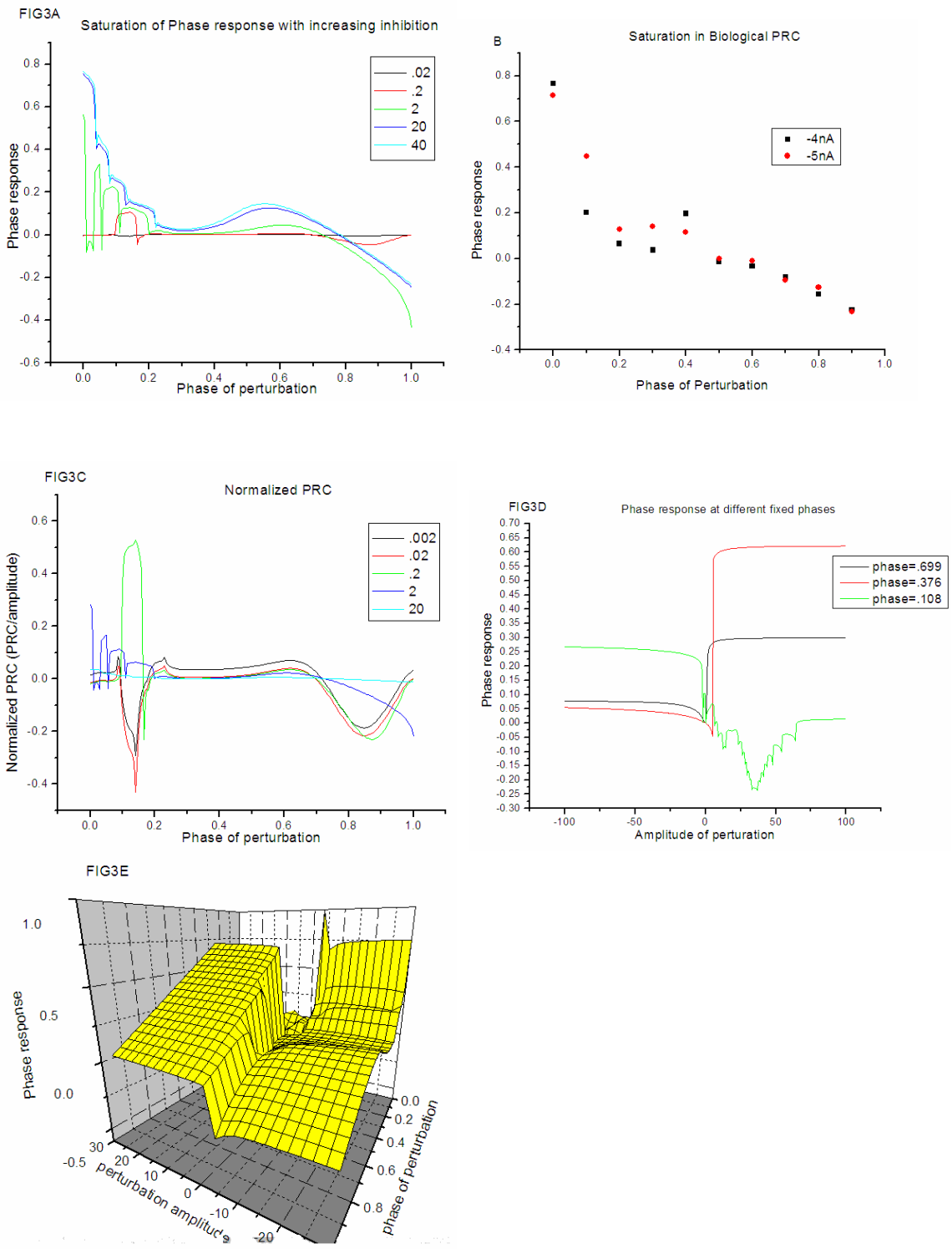

FIG 3: (**A**) Plot shows that the phase response saturates with increasing amplitude for the model neuron. Note again that during the active phase of the oscillations, perturbations cause a phase delay (i.e. negative phase shifts) but with increasing inhibition, perturbations cause an advance. (**B)** Plot shows saturation of phase response as in (a) but for the biological neuron. (**C)** We normalize the phase response in (b) by the amplitude to

facilitate comparison between different amplitudes. (**D**) Plot shows phase response at three different fixed phases as a function of amplitude. In the limit of large perturbations (positive and negative), each curve asymptotes to a horizontal line. The green curve corresponds to a phase of perturbation in the active phase of the oscillation. This was computed for the model neuron. (**E**) Multi-dimensional plot of the phase response as a function of phase and amplitude of perturbation to the model neurons.

SECTION III

Spike Deletion, Spike Addition and Burst Truncation: Given the general qualitative agreement between the PRCs of the model and biological neuron, we focus mainly now on the model neuron to try to understand the factors that determine its phase response. We observed that for strong perturbations, the phase response is due mainly to spike addition, spike deletion and burst truncation. As we have said before, spike addition is the elongation of the active phase of the oscillator as a result of the perturbation. This elongation is as a result of the appearance of new spikes (action potentials) in the active phase. Spike deletion is the shortening of the active phase caused by a reduction in the number of action potentials in the active phase. Burst truncation is a termination of the active phase by a perturbation given in the active phase. Burst truncation is, of course, accompanied by a reduction in the number of action potentials. However, burst truncation, as we have defined it, differs from spike deletion mainly in that the perturbations that cause burst truncation can only be given in the active phase, while we cannot exclude the possibility of a perturbation in the silent phase causing fewer spikes in the following active phase.

These phenomena are illustrated in Fig 4. We observed that both intermediate strength inhibition and strong excitation can cause spike addition (Fig 4 b&f). Interestingly though, the mechanisms appear to be different. In the case of inhibition (4b), there is a long delay, almost of the order of the duration of the active phase, between the 3^{rd} and 4^{th} spikes followed by an extra spike. In this case, the perturbation was given during the active phase. In phase space (not shown), the trajectory actually moves backwards in a straight line and then traces out previous spikes. As Fig 4c shows, making the distinction between a burst truncation and a spike deletion can be difficult. This situation is peculiar because there is a long period in which there are no spikes and after which the active phase begins. Fig 4d shows the situation just described in phase space. The red curve corresponds to the trajectory after perturbation. This trajectory moves backward during the long period corresponding to no action potentials and then finally makes a transition to the active phase.

Spike addition by strong excitation appears to show a different mechanism behind it. In phase space, the perturbed trajectory (red curve in Fig 4e) makes extra windings before transiting to the silent phase. More so this transition point is seen to be different from the transition point of the unperturbed trajectory (black curve). This ‘jump down’ point, in the case of no perturbation, is determined by a bifurcation value of the slow variable (Ca^{2+}). It is typically the maximum value of the slow variable. Fig 4g shows that this maximum has increased suggesting that change of the jump down point is responsible for the extra windings of the trajectory in phase space. Thus, we see that understanding how perturbations affect the transition from active phase to silent phase and vice versa will help us understand the phase response of the neuron.

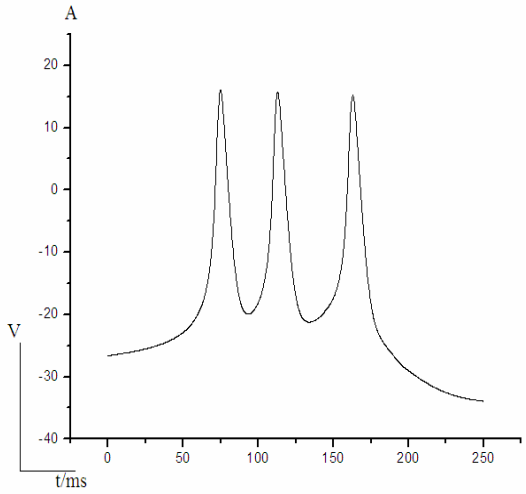
A
20
10
0
-10
-20
-30
-40
V
0
50
100
150
200
250
t/ms

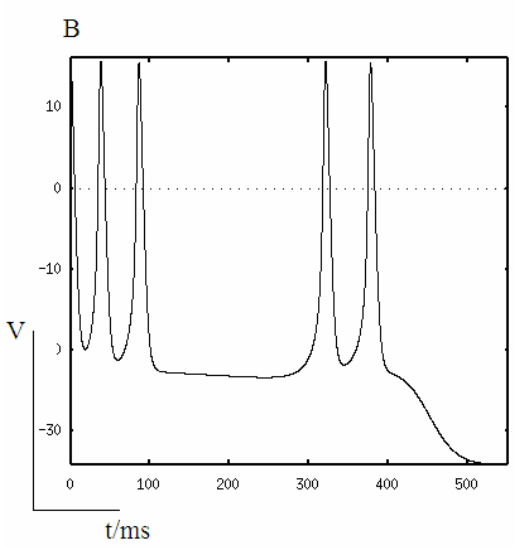
B
10
0
-10
V
-30
0
100
200
300
400
500
t/ms

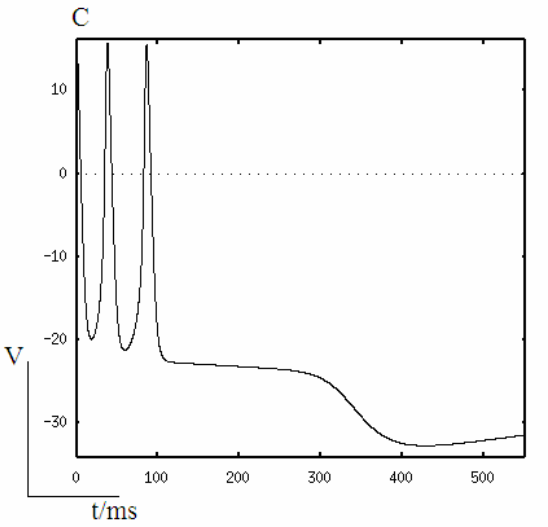
C
10
0
-10
-20
-30
V
0
100
200
300
400
500
t/ms

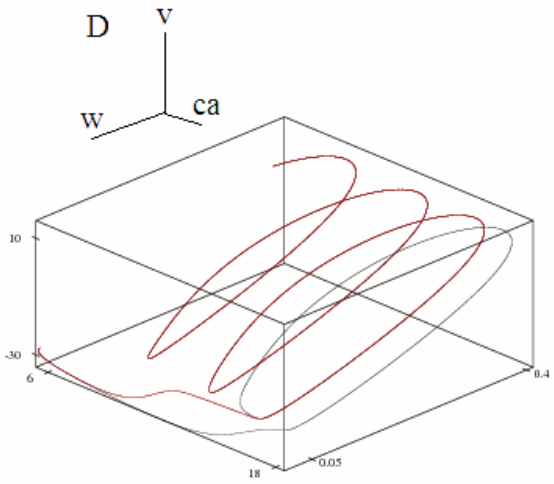
D
v
w
ca
10
-30
6
18
0.05
0.4

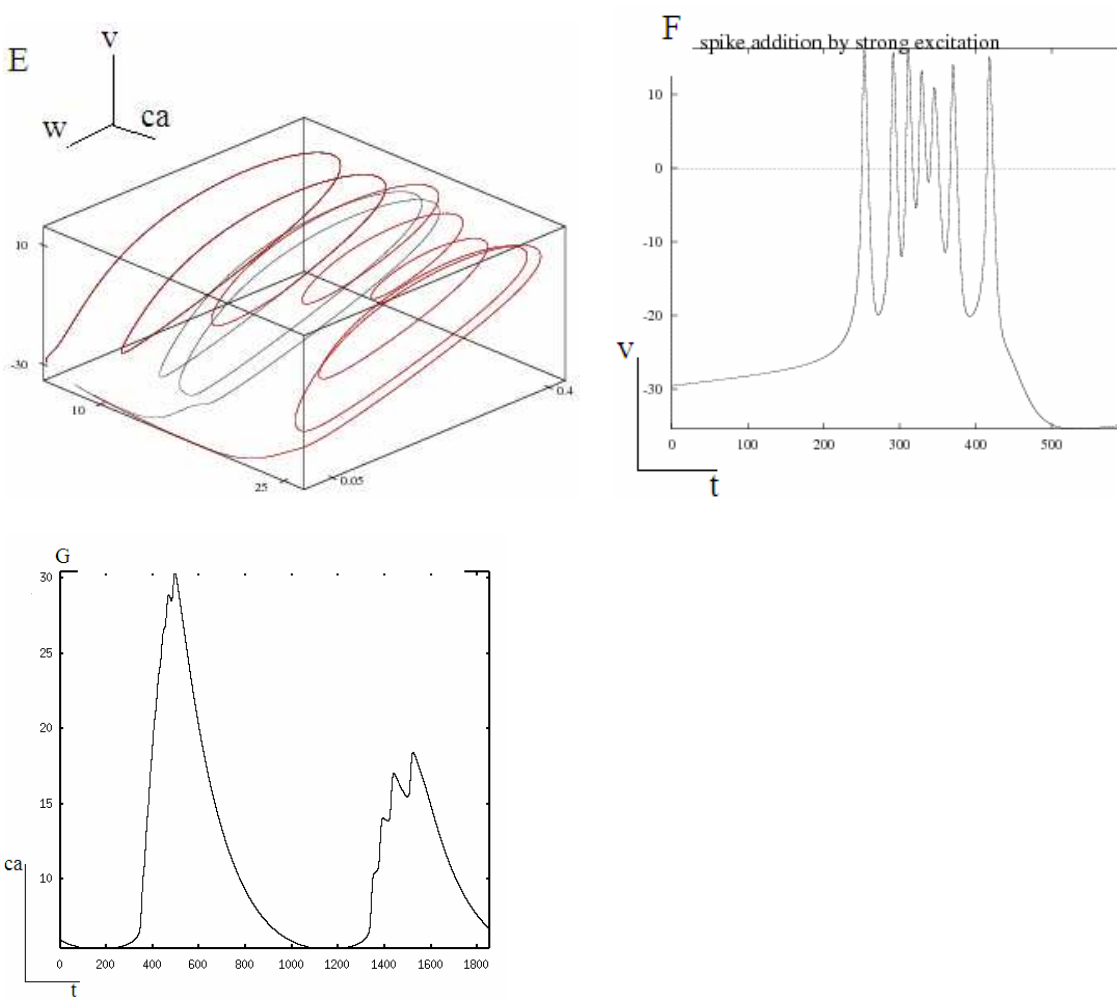

FIG 4: (**A**) Spike deletion. (**B**) Spike addition due to inhibition. Note the elongated interval between spikes 3 and 4. In phase space (not shown), the trajectory traces a horizontal line after the 3rd spike and then traces the same spikes. (**C**) Burst truncation due to inhibition in active phase. In fact, burst truncation can only be caused by inhibition. However this burst truncation is on the borderline of spike addition in (b). (**D**) Trajectory in phase space corresponding to (c). The red curve is the trajectory resulting from the perturbation and the black curve is the unperturbed trajectory. (**E**) Phase space trajectory corresponding to spike addition by strong excitation in active phase. The black curve is the unperturbed trajectory. Note that the perturbed trajectory (red trace) makes multiple windings and that the jump down point of the trajectory has been moved. (**F**) Trace of voltage corresponding to (e). (**G**) Trace of the slow variable, Ca^{2+}, showing that its maximum value, which corresponds to the jump down point, has been increased.

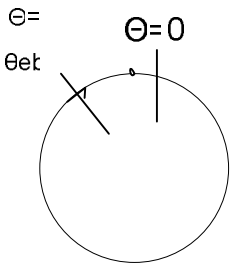

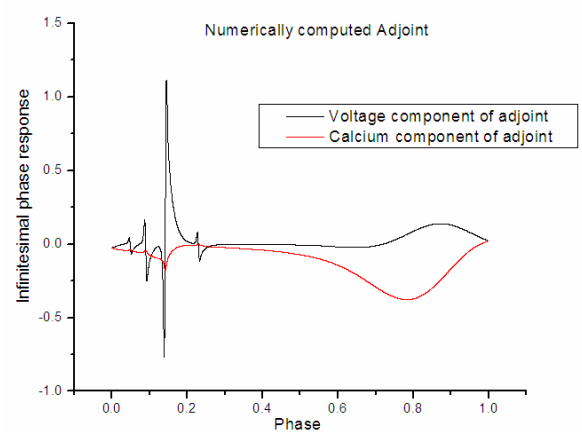

We try here to derive a priori conditions on the amplitude of the current to cause spike addition and deletion. To begin, we assume the model permits a phase description (i.e. there is a mapping of the limit cycle onto S^1, the circle). Each point on the circle corresponds to a particular phase of the oscillator. However this phase is not represented by a single point on the limit cycle but by a family of points which is the isochron. Thus, as in [11], we can write the following phase equation:

$$\dot{\theta} = 1 + Z(\theta)I(\theta) \qquad (4)$$

Here $Z(\theta)$ is the adjoint or infinitesimal PRC and $I(\theta)$ is the perturbatory input usually in the form of a square pulse. Setting the input to zero corresponds to periodic bursting as is expected. Let θ_p be the phase of perturbation, and θ_f be the phase point after perturbation where $\theta_p \in [0, \theta_{eb}]$; θ_{eb} being the phase at the end of a burst (without any perturbation). Essentially then, we are considering only perturbations that occur in the active phase. If we are going to have spike addition, it would seem necessary that $\dot{\theta} < 0$ for some interval of time so that the phase point traces out old values again thus allowing for the possibility of tracing the older spikes again. This is the situation shown in Fig 4b. To rule out the possibility of spike addition we should require that $\dot{\theta} > 0$ for $\theta \in [0, \theta_{eb}]$. This simple requirement implies that

$$Z(\theta)I(\theta) > -1 \qquad (5)$$

We must point out here that this phase description is valid only when perturbations do not cause too much deviation from the unperturbed limit cycle. Thus the situation in Fig 4e will not be allowed. The reason is that it is not clear how the change in the jump down point will affect the isochrons. The violation of (5) explains why intermediate inhibition can cause spike addition (Fig 4b) and weak perturbations do not. Strong inhibition invariably causes burst truncation.

Going along with this analysis, let $0 < \theta_p < \theta_f < \theta_{eb}$. Define: $\zeta = \frac{ISI_{\max}}{T}$ where $ISI_{\max}$ is the maximum inter-spike interval in the unperturbed burst and *T* is the period of the entire oscillation. To guarantee spike deletion we require that $\int_{\theta_p T}^{\theta_p T+\tau} \dot{\theta} dt = \zeta$ (τ is the duration of the perturbation) which is a way of saying that $\theta_f - \theta_p = \zeta$. This is a reasonable requirement because it says that the final phase point is one spike away. Thus we get:

$\int_{\theta_p T}^{\theta_p T+\tau} (1 + Z(\theta) I(\theta)) dt = \zeta \Rightarrow \int_{\theta_p T}^{\theta_p T+\tau} (Z(\theta) I(\theta)) dt = \zeta - \tau$. Multiply both sides by τ^{-1} and using the average value theorem of calculus and redefining $I(\theta)=I_p$ we obtain that:

$$\langle I_p Z \rangle = \frac{\zeta - \tau}{\tau}$$

Assuming that the perturbation is a square pulse we can obtain the following

$$I_p = \frac{\zeta - \tau}{\tau \langle Z \rangle}$$

This gives a parameterization of the perturbation current by the duration of the perturbation with $\tau \neq \zeta$. For fixed non-zero current you can also determine duration of perturbation. We now have sufficient conditions for spike deletion (and with minor modifications, spike addition).

SECTION IV

Breaking apart the Phase Response Dynamics: In order to better understand the phase response dynamics of the neural oscillator, we study the PRC of the oscillator over the active and silent phases of the oscillation separately and then piece them together obtain the full response. In so far as such piecemeal operation is possible, one fundamental assumption that has to be made is that the perturbations given to the oscillator in the silent phase for example, will only advance or delay the start of the following active phase without drastically affecting the events, i.e. spikes, in the active phase. As we have indicated, strong perturbations, for instance, can cause spike addition by increasing the jump down value. Hence, we explicitly exclude strong perturbations from our considerations here. Furthermore, we assume that perturbations given in the silent phase will not cause spikes to be added or deleted and more so will not change the relative timing of the spikes in the active phase. This seems like a reasonable assumption in so far as we do not perturb too close to the transition from the transition from active to silent phase or vice versa. Likewise, we assume that perturbation in the active phase do not affect passage in the silent phase.

We would like to point out here some of the possible virtues in utilizing such a method to reconstruct the PRC. If we were to analyze networks of bursting coupled neurons, it seems clear that there are different types of synchronization that may occur [2, 13]. Neurons may become synchronized in their active phases, i.e. the spikes in the active phase will become phase locked. Their resting states my also synchronize without having their active phases synchronize. Other different possibilities abound. The upshot is that in order to understand such network behavior, it may become necessary to perform such a dissection of the PRC.

Our old method of computing the PRC can be described for purpose of the discussion here as measuring the change in timing of the *next* active phase in the ongoing perturbation. We call this method M1 to facilitate our discussion. The first method (M2 for short) we propose is to compute the PRC by perturbing in the active phase and then measuring the change in timing of the end of the *current* active phase. More precisely, set the RE to be the start of the active phase and assign a phase of zero to this point. Let T_{eb} be the time of the end of the active phase of the unperturbed neuron as measured from the RE. Let t_{p} be the time of the stimulus as measured from the RE. Denote as $T_{\mathrm{eb,\,new}}$ the time of the end of the active phase after the stimulus. Then $\Delta T_{\mathrm{eb}=} T_{\mathrm{eb}} - T_{\mathrm{eb,\,new}}$ will be the change due to the perturbation. We then wish to use ΔT_{eb} (after normalization by the period of the entire oscillator, which is the sum of the duration of active and silent phases) as an estimator for the PRC using M1 at least for perturbations that occur in the active phase. If what we have said above about the interaction between both phases is granted, then it seems reasonable that M2 should agree closely to M1 used previously, a method widely used by experimentalists and theoreticians alike. The following figures shows that the two methods do indeed agree for perturbations considered.

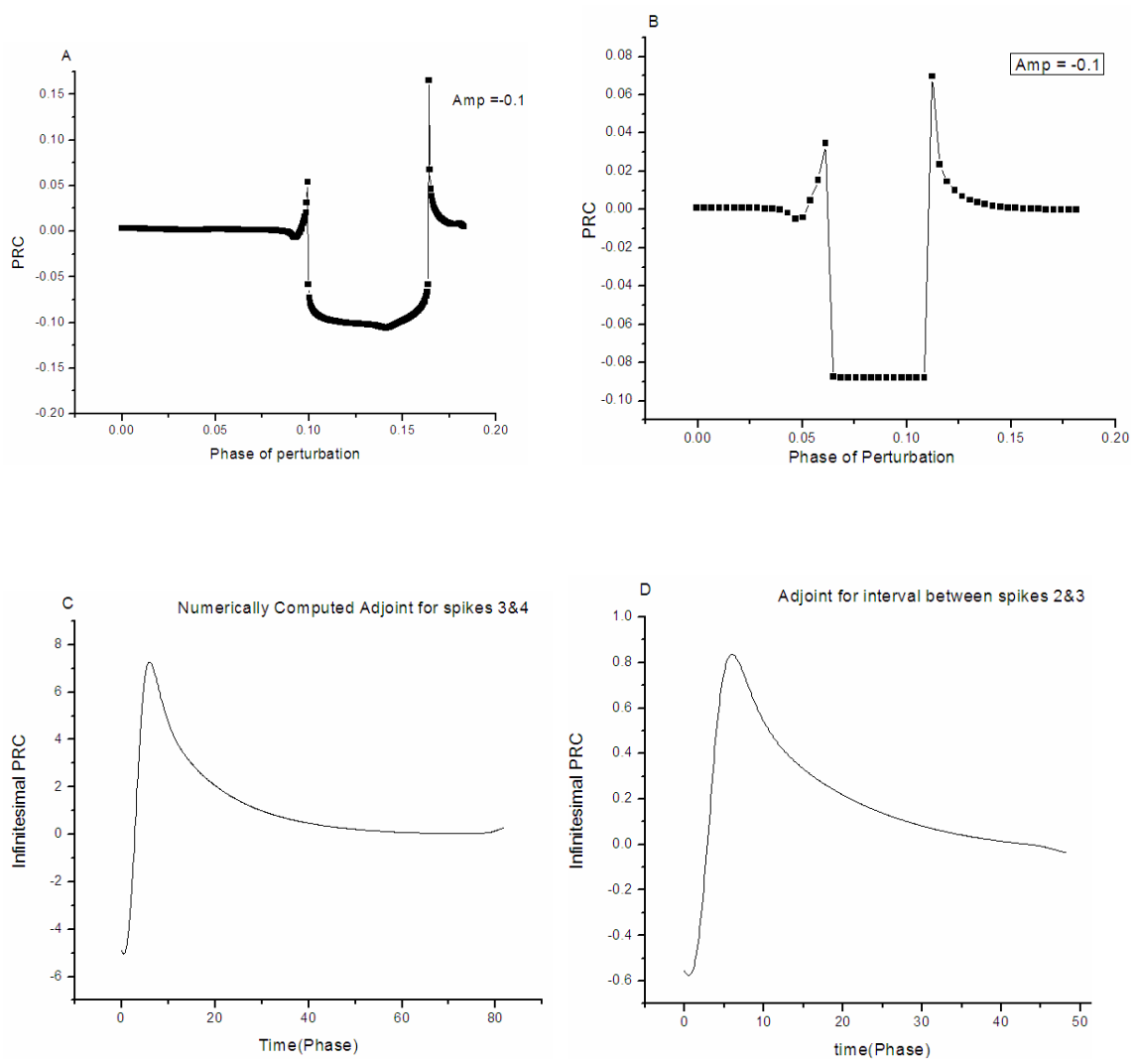

FIG 5: (**A**) The PRC computed for a perturbation of -0.1 using M1 outlined above. (**B**) PRC computed using M2. Note the qualitative similarity between (a) and (b). This suggests that M2 is a good approximation to M1. (**C**)-(**D**) Numerically computed adjoint or infinitesimal PRCs for the 2^{nd} and 3^{rd} inter spike intervals of the oscillation respectively. Note the qualitative similarity. Both infinitesimal PRCs have been plotted against their periods.

We then proceeded to further dissect the active phase by trying to reconstruct the PRC for perturbations between each spike in the burst and then trying to use this predict the PRC again. The idea is that since the infinitesimal PRCs are nearly identical (Fig 5 c&d), perturbations given in each inter spike interval delay the timing of the spikes in a predictable fashion. Since we know that the phase response is due mainly to the shifting of the relative spike times, we can thus predict the phase response of the neuron by simply understanding how two consecutive spikes shift relative to perturbations. We briefly outline one method and its shortcomings here and refer the details to the companion paper [18].

The main idea is that perturbations which occur after the *i*th (*i= 1, 2, 3)* spike shifts the timing of the (*i*+1) st spike without changing the *relative* timing of the subsequent spikes. If this would be so, then the perturbation will cause only the following spike to be shifted while the rest are simply translated. This gives us a way to predict the timing of the end o the burst, and, then, using the results above, we can then determine the PRC. We can do this because we know M2 to be able to predict M1, thus since the shift in the spike immediately following the perturbation will translate to a shift in the end of the active phase, we thus have an approximation to M2 which we know approximates M1, our original method. The results of this method, which we call M3, are summarized in [18]. We note however that this method is only approximate because perturbations may or may not transmit the spike shifting linearly through the different inter spike situation. Two representative case of nonlinear shifting are shown in Fig 6 below.

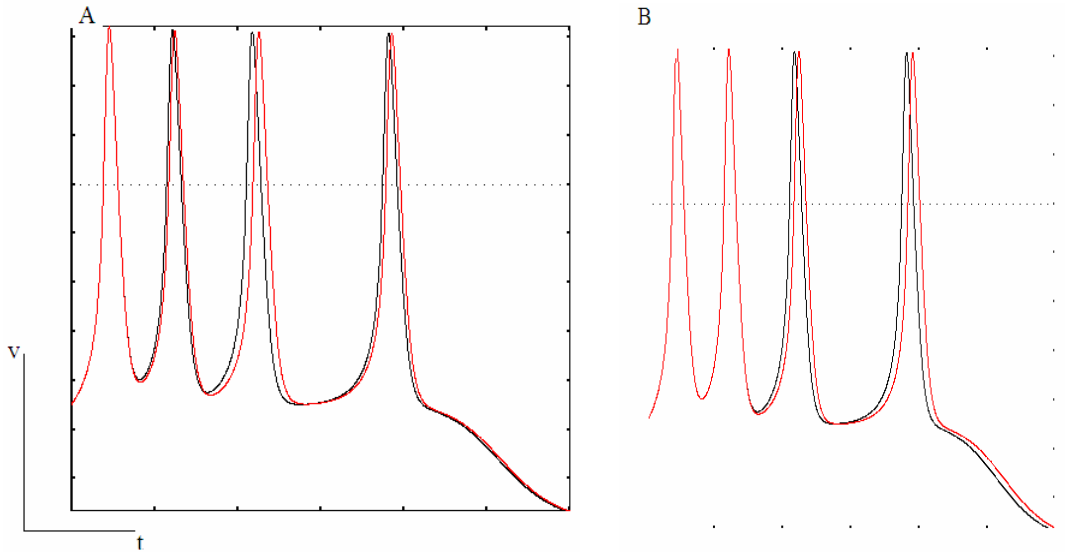

Fig 6 above shows how the spike time shifts that occur in the active phase may vary nonlinearly with the inter spike intervals. In 6a, the perturbation is given in the first interval and the perturbed voltage trace (red curve in figure) has its second spike shifted relative to the unperturbed trace (black curve). The third spike shows an even greater shift while the fourth spike shows a smaller shift. Thus the assumption that the shift is

translated linearly may fail to hold. In 6b, the perturbation is given in the second inter spike interval. It causes the third spike to occur later than it would have without a perturbation. The fourth spike shows a shift much bigger than that seen in the third spike thus indicating that the effect of the perturbation is compounded nonlinearly.
It may turn out that determining or even approximating the nonlinear nature of the spike shifting will be non trivial. However, we are working on two possible methods of figuring out how perturbations change the inter spike intervals and hence the timing of the spikes. The first method then can be briefly described in words as this: we record the different inter-spike interval duration without any perturbation. For discussion purposes suppose that a perturbation is delivered in the first ISI. We can use the adjoint or PRC to determine by how much the second spike will be shifted. We can then use this shift and the *same* PRC to predict the timing of the third spike and so on. The idea is to compound the effect of one perturbation through out the active phase.
The third method is more mathematical in the sense that it uses ideas from bifurcation theory. We again describe the method in words leaving the details to future work. The active phase corresponds to spiking due to the fast subsystem of the differential equations (see section v below). This fast spiking activity terminates due to a saddle homoclinic bifurcation of the periodic orbits corresponding to spiking. Close to this bifurcation value, the system can be described by so called reduced models or normal forms [2]. Hence we obtain the reduction:

$$V = f(V, Ca(\theta t))$$
$$Ca = Ca(\theta t)$$

The two equations above are decoupled from each other, which helps us in out analysis. Θ represents factor which might influence the time scale of evolution of the Ca^{2+} equation. Further more, close to this bifurcation we have that the (instantaneous) frequency of the periodic orbits depends on the bifurcation parameter, which is Ca^{2+}. This dependence can be written as $freq = g(Ca)$ where g is determined entirely by the normal form for this particular bifurcation. Since the period is the inverse of the frequency, we can thus determine the inter spike period. The goal then is to determine how perturbations change g and thus the frequency and the inter spike period.

\

SECTION V

Further Analysis of Burst Truncation: We promised in the previous section to qualify the distinction between a burst truncation and a spike addition. In order to do this and more we resort here to geometric singular perturbation theory. This discussion here closely follows that in [3] although we adapt the discussion here with the aim of explaining burst truncation. Burst truncation is harder to analyze without imposing extraneous conditions on the phase model. To explain burst truncation as well as give possible insights into why the PRC saturates, we use here elements from dynamical systems theory. The main assumption here is that there is a clear separation of time scales in which two distinct but interrelated systems evolve. The idea is to construct a special solution as one that periodically visits the invariant manifolds of the fast subsystem. We can generically write the equations as due to the general setting of the problem:

$$\dot{x} = f(x, y, z) \qquad (6)$$
$$\dot{y} = g(x, y, z) \qquad (7)$$
$$\dot{z} = \varepsilon h(x, y, z) \qquad (8)$$

With ε small as usual and (3&4) forming the fast subsystem (FS). Furthermore we assume as usual that the FS has a cubic shaped line of fixed point as shown below:

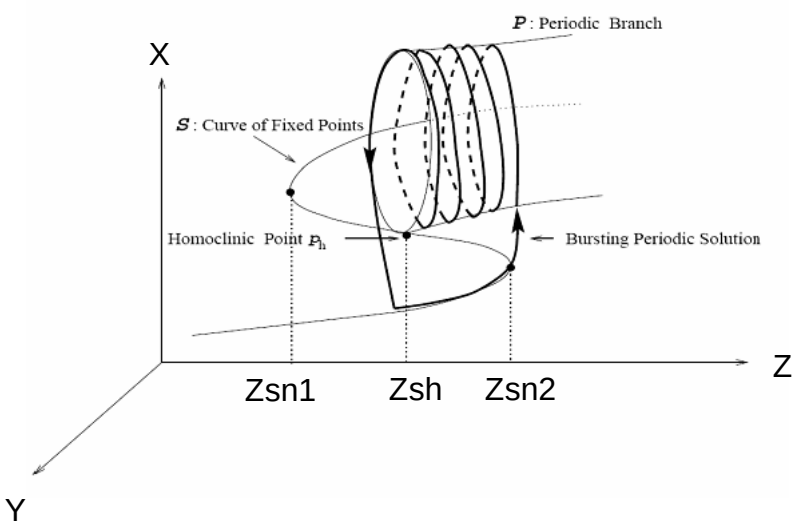

Z here represents calcium in our model and is the slow variable. We let Z_{SH} correspond to the value at which a saddle-homoclinic bifurcation occurs in the FS. Z_{SN1} and Z_{SN2} correspond to saddle-node bifurcations. Between Z_{SH} and Z_{SN2} the FS is bi-stable. It is this bi-stability that enables bursting behavior since the slow variable modulates how

trajectories visit the attracting invariant sets of the FS. What interests us immediately is the middle-branch which we assume is made of saddle points. To each saddle we can ascribe stable and unstable manifolds, W^s and W^u respectively. If we take the union of these manifolds we get W^s_{tot} and W^u_{tot}. These manifolds are uniquely and clearly defined in the case where ε = 0. However, it is shown in [3, 14] that these manifolds still persist for ε small but positive. Usually, one transitions from the active phase (spiking) to the rest phase via the homoclinic bifurcation however, while in the bi-stable region, we can transition from the active phase to resting by having perturbation push us past W^s_{tot} which separate the two regimes. This would be an instance of burst truncation. Perturbations that push us into such regimes will be called strong perturbation. Thus we see that W^s_{tot} forms a sort of threshold for perturbations and determines if a perturbation will cause a truncation or not. We computed the limiting values of inhibition at and beyond which there was a burst truncation. The idea is simple: we send increasing inhibitory perturbations at a fixed phase in the active part of the oscillation and the value of the inhibition at which a truncation is first observed to occur is the threshold value. We note that this threshold is not the (voltage) threshold that is the stable manifold we have described above, but it is related to it. The actual stable manifold can be computed as outlined in [20]. The qualitative result of our computation is shown below:

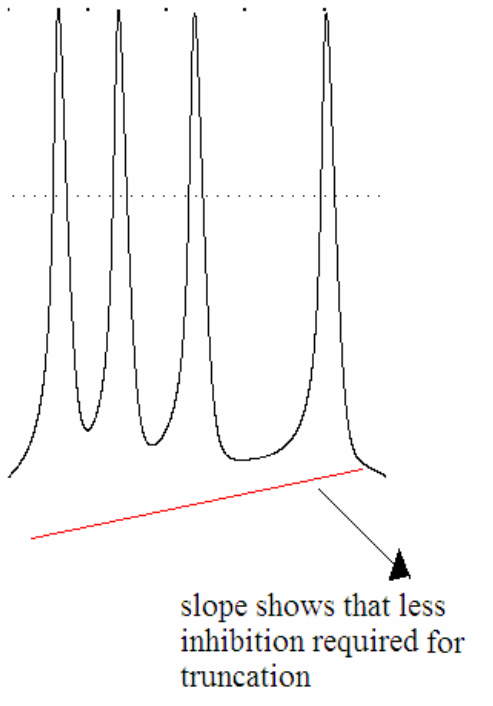

We can use this to explain the saturation in the PRC. The main idea is that if strong perturbation which pushes the orbit from the active phase past W^s_{tot}, the orbit is then carried into the basin of attraction of the lower branch of stable fixed point and hence into the active phase. Hence sufficiently large (and brief) perturbations all have the same

effect of carrying the orbit into the lower branch. In order to quantify this description, we can attempt to reduce the dynamics to that of the slow variable for strong perturbations and then use this to measure the PRC. The basic assumption then is that after we give a strong perturbation in the active phase, the slow variable does not change much. If we assume that the lower branch is very strongly attracting, we than then say that the trajectory tracks the lower branch almost as soon as the perturbation is given and thus we land very close to the original limit cycle. Thus we need only to follow Z as it varies between Z_{SH} and Z_{SN2} to predict the next jump points and hence the start of the next burst. We must add that in reality the time it takes some time to get close to the lower branch again. The time is can be reasonably assumed to be small for perturbations given in the active phase. However, perturbation in the silent phase require some time for the orbit to return to the original limit cycle, for if not perturbations given during the silent phase will cause essentially no phase shifts and we know from the figures above that this is not the case. How then do we explain the saturation of the PRC for perturbations in the silent phase? We hypothesize that because the perturbations occur for some fixed duration, the time it takes to get close to the lower branch can be related to the (exponential) rate of attraction to the lower branch. Since this rate is bounded, the time it takes to get close to the lower branch is also bounded. Note that this analysis then implies that strong perturbations of different durations will saturate but to different values.
To cement this idea of tracking the dynamics of the slow variable alone, we turn to a crude implementation. Shown below is the trace of the calcium variable over one period of the burst. To make the analysis easier, we fit this trace with exponentials and redefine the dynamics of the calcium variable depending on whether it is in the active or silent phase. This allows us to derive simple equations for the PRC making it analytically tractable. We assume that the slow equations can be written as:

$$\dot{Z} = \lambda_1 Z \text{, if } 0 \le t \le T_{eb} \qquad (9)$$

$$\dot{Z} = -\lambda_2 Z \text{, } T_{eb} \le t \le T \qquad (10)$$

Here $\lambda_1, \lambda_2 > 0$ and are determined uniquely by the boundary conditions

$$Z(0) = Z_{SN2}$$
$$Z(T_{eb}) = Z_{SH}$$
$$Z(T) = Z_{SN2}$$

Everything is as defined before but here *T* is the period of the unperturbed neuron. Let t_p be the time of perturbation and furthermore let $t_p \in [0, T_{eb}]$. Since we assume that orbit is pushed to the lower branch at the same value of the calcium variable, Z. we denote as t', the time at which $Z = Z_{SN2}$. This time will correspond to the "jump up" time. Using (10) we can write an exact equation for this time:

$Z_{SN2} = \Phi_1(t_p) e^{-\lambda_2 t'}$, which yields that;

$$t' = -\frac{1}{\lambda_2} \ln\left(\frac{Z_{SN2}}{\Phi_1(t_p)}\right).$$

Here $\Phi_1(t_p)$ is the solution of (9). Denote as t'' the time of the start of the next active phase as measured from the start of the current active phase. It is clear that $t'' = t_p - t'$. Putting it all together we obtain the that phase shift (PR in the formula) due to this perturbation is given by"

$$PR = \frac{1}{T}(T - t'')$$

The results of this computation are shown in the figure below. The PRC obtained is seen to be a straight line and it can be shown that the slope of this line depends only on λ_1 and λ_2. In fact, one could extend this method of tracking the slow variable to explain the saturation of the PRC with increasing excitation in the silent phase. In this case, however, we do not have a burst truncation. The situation then is that strong perturbations given in the silent phase pushes the trajectory in to the active phase. It is this start of the active phase we measure as the phase response and it should be clear then that it should result in a straight line since the start of the active phase is essentially at the instant of perturbation. This explains the red curve in Fig 2c and further suggests that the discontinuity is not an artifact but a topological property of the PRC.

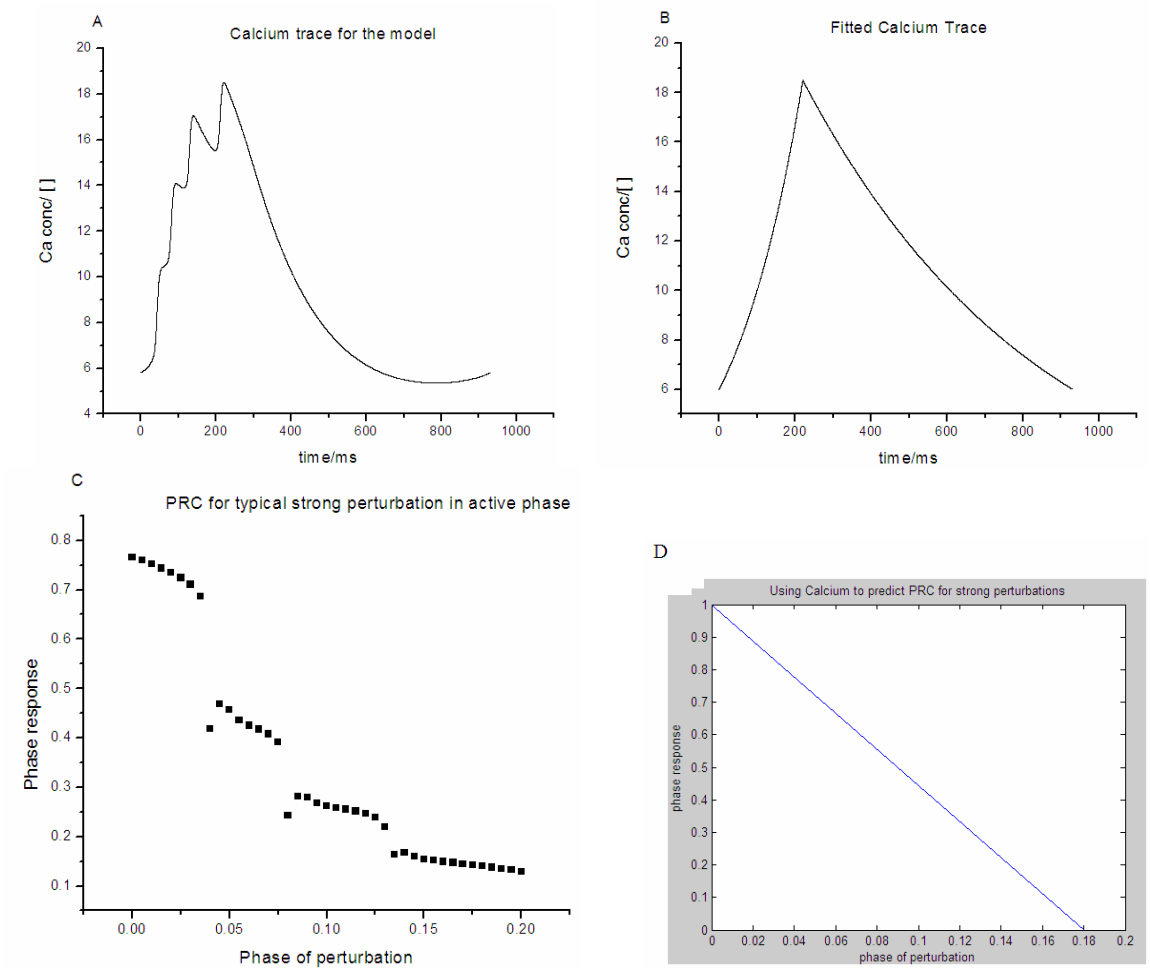

(**A)** Trace of the Ca^{2+} concentration for one period of the oscillation. (**B**) Plot showing the piecewise exponentially fitted Ca^{2+} concentration for one period of oscillation. (**C**) PRC of model neuron for perturbations in the active phase. Increasing amplitude only saturates this curve. Discontinuities occur at the peak of the action potentials in the active phase. (**D**) Analytically determined PRC shows that for strong perturbations, the phase response is essentially linear. This slope of this line is roughly equal to the average slope of that in (c). Not however, that there are no discontinuities. This is due to the smoothness of the fitting.

Discussion, Conclusion and Future Directions

Our numerical and theoretical studies, though far from complete, give us some insight to the mechanisms determining the sensitivity of the neuron to perturbations. The response has been shown to be qualitatively different depending on whether we have strong or weak perturbations and depending on whether we perturb in the active or silent phase. We also showed that much of the phase response for strong perturbations is due to spike addition, spike deletion and burst truncation. For weak perturbations in the active phase, the phase response is caused by a shift in the timing of the spikes. Strong perturbations cause burst truncation or spike addition depending on if it is inhibitory or excitatory and depending on the phase. The results are summarized in the following table:

Strength / Phase of Perturbation.	Weak Perturbations	Intermediate Perturbations	Strong Perturbations
Active Phase	Shifting of spikes (Inhibition and Excitation)	Inhibition can cause spike addition and delayed burst truncation.	Burst Truncation (Inhibition) Spike addition and Increase in Jump down point (Excitation)
Silent Phase	Little effect with the most sensitivity at late phase (Inhibition and Excitation)	Little effect with the most sensitivity at late phase (Inhibition and Excitation)	Excitation causes active phase to begin abruptly. In late phase, can also cause spike addition

Thus we can see how two coupled bursting neurons considered in [8] would be likely to exhibit anti-phase synchrony if they are coupled strongly by inhibition. This anti-phase synchrony is due to burst truncation so that one neuron being in the active phase will preclude the possibility of the other neuron also being in the active phase.

To our knowledge, it is still an open question how one could use PRCs to predict other different types of synchrony. We proposed the new methods of constructing the PRC as a first step towards this and other goals. However, the method we developed in [18] is only a first order approximation. We still need an algorithm that predicts the timing of the spikes in the active phase given only the PRC between two consecutive spikes. As we showed above the spike shifting is nonlinear. We are currently working on a method in which the spike shift is compounded from one inter spike interval to another using only one PRC since we have shown them all to be equivalent above.

We also predict that the effect of spike addition will become pronounced when one considers networks of coupled oscillators. As the above table indicates, spike addition is occurs because there is a change in the jump down value of the slow variable. Thus a more intricate analysis needs to be performed to understand how strong excitation or intermediate inhibition changes the jump down value. If this jump down value can be at least approximated then we can perform an analysis similar to that in Section v where we reduce the phase response to tracking the value of the slow variable.

Acknowledgements
We would like to thank Farzan Nadim, Amitabha Bose and Jorge Golowasch, for guiding us through the tide that is research through useful comments, suggestions and constructive criticisms. We also thank Horacio Rotstein and Victor Matveev for letting their doors open when we had questions. We will also like to acknowledge the efforts of Vahid Tohidi, Shunbing Zhao, Farzad Sheibanie and Alexander Fileus in guiding us through the experimental part of our work and providing a lively atmosphere for us to work; much of this work will not have been completed with out them. This research was supported partially by a UBM grant.

Appendix

Here is the XPP code:

```
dv/dt = ( I - ICa-(gk*w+gkca*z)*(V-VK)-gl*(V-Vl)+m*(s(t-tau)))/c
dw/dt = phi*(winf(V)-w)/tauw(V)
dca/dt=pert*eps*(-mu*Ica-ca)
tau'=0
Ica=gca*minf(V)*(V-Vca)
z=Ca/(Ca+Ca0)
v(0)=-18.7
w(0)=.071
ca(0)=10.39
minf(v)=.5*(1+tanh((v-v1)/v2))
winf(v)=.5*(1+tanh((v-v3)/v4))
tauw(v)=1/cosh((v-v3)/(2*v4))
s(t)=heav(t)*heav(sigma-t)
param vk=-84,vl=-60,vca=120
param i=45,gk=8,gl=2,c=20
param v1=-1.2,v2=18,pert=1
param m=0,sigma=50 t0=931
#param_fig1-3 v3=2,v4=30,phi=.04,gca=4.4
param v3=12,v4=17.4,phi=.06666667,gca=4
param v3=12,v4=17.4,phi=.23,gca=4
param mu=.2,ca0=10,eps=0.005,gkca=.25
aux zbar=z
aux icaa=ica
aux vprime=( I - ICa-(gk*w+gkca*z)*(V-VK)-gl*(V-Vl)+m*(s(t-tau)))/c
aux prc=1-t/t0
aux phase=tau/t0
aux amp=m
@ xp=zbar,yp=v,xlo=0,xhi=1,ylo=-75,yhi=20,total=2000,dt=1,meth=gear,toler=1e-5
@ dtmax=5,dtmin=1e-10,bound=1000
@ back=white
done
```

References and Bibliography

[1] Prinz, A., Thirumulai, V. & Marder, E., The Functional Consequences of Changes in Strength and Duration of Synaptic inputs to Oscillatory Neurons, *J. Neuroscience.*, 23 (2003) 943-954.

[2] Izhikhevic, E.M, *Dynamical systems in Neuroscience*

[3] Lee, E. & Terman, D., Uniqueness and Stability of Periodic Bursting Solutions, *J. Diff. Eq.*, 158 (1999) 48-78.

[3] Wiggins, S., *Normally Hyperbolic Invariant Manifolds in Dynamical Systems*, Springer-Verlag, New York, 1994.

[4] Perko, L., *Differential Equations and Dynamical Systems*, Springer-Verlag, New York, 2001.

[5] Coombes, S. & Bressloff, P. eds, *BURSTING: The Genesis of Rhythm in the Nervous System*, World Scientific Publishing Co., 2005.

[6] Guckenheimer, J., Isochrons and Phaseless Sets, *J. Math. Bio.*, 1 (1975) 259-273.

[7] Kawato, M., Transient and Steady State Phase response Curves of Limit Cycle Oscillators, *J. Math. Bio.*, 12 (1981) 13-30.

[8] Oprisan, S., Prinz, A. & Canavier, C., Phase Resetting and Phase Locking in Hybrid Circuits of One Model and One Biological Neuron, *Biophysical Journal*, 87 (2004) 2283-2298.

[9] Kawato, M. & Suzuki, R., Biological Oscillators Can Be Stopped Topological Study of a Phase Response Curve, *Biol. Cybernetics* 30, (1978) 241-248.

[10] Butera, R. & Preyer, A., Weak Phase-Resetting of Neural Oscillators, Proceedings of the 2005 IEEE Engineering in Medicine and Biology 27th Annual Conference, 2005.

[11] Rinzel, J. & Ermentrout, B., Analysis of neural excitability and oscillations, In *Methods in Neuronal Modeling: From synapses to Networks*, C. Koch and I. Segev, eds. 1989, MIT Press (revised 1998).

[12] Ermentrout, B. *Chapter 7: Neural Oscillator. I. Weak Coupling*

[13] Booth, V. & Bose, A., Burst Synchrony Patterns in Hippocampal Pyramidal Cell Model Networks, *Network: Comput. Neural Syst.*, 13 (2002) 157-177.

[14] Fenichel, N., Geometric Singular Perturbation Theory for Ordinary Differential Equations. *J. Diff. Eq.*, 31 (1979) 53-98.

[15] Jones, C.R.K., A Geometric Approach to Systems with Multiple Time Scales.

[16] Ermentrout, B., *Simulating, Analyzing, and Animating Dynamical Systems: A guide to XPPAUT for Researchers and Students,* SIAM, 2002.

[17] Ermentrout, B., Type I membranes, phase resetting curves, and synchrony. *Neural Comput.,* 8 (1996) 979–1001.

[18] Alborz Yarahmadi *et al*

[19] Winfree, A., *The Geometry of Biological Time*. Springer, New York, 2001. Second Edition.

[20] Osinga, H. & England, J., Separating Manifolds in Slow-Fast Systems, ENOC-2005, Eindhoven, Netherlands, 7-12 August 2005.